

# Identification of circular RNA\_0000919 as a potential diagnostic and prognostic biomarker of tongue squamous cell carcinoma using circular RNA microarray and reverse transcription-quantitative PCR analyses

HONGLI LIU, QI LI, HAN QI, FENGZHI DU and YANLI QIU

Department of Stomatology, Cangzhou Medical College, Cangzhou, Hebei 061001, P.R. China

Received January 12, 2021; Accepted May 25, 2021

DOI: 10.3892/ol.2022.13390

**Abstract.** The present study aimed to identify differentially expressed (DE) circular RNAs (circRNAs/circs) using microarray analysis and to further explore the clinical significance of 10 candidate DEcircRNAs in patients with tongue squamous cell carcinoma (TSCC). A total of 60 patients with TSCC who underwent surgery were enrolled and five pairs of TSCC and adjacent (Ctrl) tissues were used for circRNA microarray analysis. Subsequently, the top five upregulated and downregulated DEcircRNAs were detected by reverse transcription-quantitative PCR (RT-qPCR) analysis in 60 pairs of tumor and Ctrl tissues, and their association with tumor features and overall survival (OS) was further analyzed. circRNA expression was used to differentiate TSCC from Ctrl tissues by principal component and heatmap analyses. A total of 134 upregulated and 67 downregulated DEcircRNAs were identified in TSCC tissues compared with Ctrl tissues. The DEcircRNAs were enriched in oncogenic signaling, including the 'Wnt signaling pathway' and the 'MAPK signaling pathway'. The majority of DEcircRNAs exhibited several target microRNAs (miRNAs) in regulatory network analysis. These findings were validated by RT-qPCR analysis and the results demonstrated that the expression levels of 9/10 selected candidate DEcircRNAs (circ\_0020048, circ\_0000919, circ\_0004525, circ\_0002113,

circ\_0004029, circ\_0004503, circ\_0008752, circ\_0002300 and circ\_0001811) were dysregulated in TSCC tissues compared with Ctrl tissues. The expression levels of five DEcircRNAs (circ\_0004503, circ\_0008752, circ\_0002300, circ\_0020048 and circ\_0000919) were associated with pathological grade or tumor clinical stage. Notably, only the expression levels of one DEcircRNA (circ\_0000919) were associated with decreased OS. In conclusion, the present study indicated aberrant circRNA expression and potential circRNA-miRNA interactions in TSCC and identified circ\_0000919 as a diagnostic and prognostic biomarker for TSCC management.

## Introduction

Tongue squamous cell carcinoma (TSCC) is one of the most common (90%) oral squamous cell carcinomas and it is estimated to be responsible for 300,000 newly diagnosed cases and 130,000 cancer-associated deaths worldwide every year (1,2). Its prevalence is 0.12 per 1,000 individuals in Asia (1,2). TSCC generally occurs in the middle-aged male population and the major etiological factors for this disease include tobacco use, alcohol consumption and betel nut chewing (3,4). The majority of TSCC cases are noted on the lateral border of the tongue and the clinical manifestations of this condition consist of pain, burning sensation and swallowing difficulties (5,6). Despite the improvements made in TSCC therapy, such as surgical resection, radiation and chemotherapy, the 5-year survival rate of patients with TSCC was reported to be ~50% worldwide in 2016 due to delayed diagnosis, locoregional recurrence and distant metastasis of the tumors (4,6). Therefore, it is essential to identify novel and promising biomarkers for the early screening and follow-up of patients with TSCC.

Circular RNAs (circRNAs/circs) are a specific type of endogenous non-coding RNAs with covalently closed loop structure, which are ubiquitously expressed in various cell types including cancer cells, immune cells, hematopoietic stem cells etc. (7,8). Accumulating evidence has revealed that circRNAs exhibit multiple biological functions, including as microRNA (miRNA/miR) sponges and regulators of transcription, splicing and translation (7,8). They are involved in diverse biological processes, including induction of epithelial-mesenchymal transition (EMT), regulation of angiogenesis, activation

---

*Correspondence to:* Dr Hongli Liu, Department of Stomatology, Cangzhou Medical College, 1 and 3 Laboratory Building, 39 Jiuhu West Road, Cangzhou, Hebei 061001, P.R. China  
E-mail: luolinhao985825@163.com

*Abbreviations:* circRNA, circular RNA; Ctrl, adjacent tissue; DEcircRNA, differentially expressed circRNA; EMT, epithelial-mesenchymal transition; FC, fold change; GO, Gene Ontology; KEGG, Kyoto Encyclopedia of Genes and Genomes; OS, overall survival; PCA, principal component analysis; RT-qPCR, reverse transcription-quantitative PCR; TSCC, tongue squamous cell carcinoma

*Key words:* circRNA, TSCC, microarray and bioinformatics analyses, RT-qPCR, OS

of oncogenic signaling and TSCC progression (7-10). For example, a previous study by Yao *et al.* (11) demonstrated that circ\_0001742 expression is increased in TSCC tumor tissues compared with the corresponding levels noted in adjacent (Ctrl) tissues. Furthermore, high expression levels of circ\_0001742 in tumors are associated with higher TNM stage and decreased survival rate in patients with TSCC (11). Additionally, it has been demonstrated that circ\_081069 expression is upregulated in TSCC tissues compared with the corresponding expression levels noted in Ctrl normal tissues (11). Furthermore, its upregulation increased the proliferative and migratory abilities of TSCC cells (12). These studies indicated the potential roles of specific circRNAs in the pathological evaluation of TSCC (11,12). However, to the best of our knowledge, the comprehensive circRNA expression profile in TSCC has not been fully investigated. Therefore, the present study aimed to identify differentially expressed (DE) circRNAs in TSCC tissues compared with paired Ctrl tissues using microarray analysis, to further validate the expression levels of 10 candidate circRNAs, and to examine their association with tumor features and survival in patients with TSCC.

## Materials and methods

**Patients.** The present study included 60 patients with TSCC who were recruited between January 2017 and December 2019 and underwent surgery at the Oral Medicine Department of Cangzhou People's Hospital (Cangzhou Medical College, Cangzhou, China). The patients were eligible for analysis in the present study if they met the following criteria: i) Diagnosis of TSCC confirmed by pathological examination; ii) aged >18 years old; iii) surgical resection as primary treatment; iv) availability of fresh-frozen tumor and paired Ctrl tissues; and v) availability of main clinical data for study analysis. The patients were excluded according to the following criteria: i) Neoadjuvant therapy prior to surgery; ii) complications due to other malignant tumors; iii) known acquired immune deficiency syndrome; and iv) missing survival follow-up records. Written informed consent was provided by each eligible patient or his/her guardian if the patients were dead when the clinical data was collected. The present study was approved by the Ethics Committee of Cangzhou Medical College (approval no. 20190611-3; Cangzhou, China).

**Specimen collection.** The tumor tissues and paired Ctrl tissues from each enrolled patient were collected from the specimen room of Cangzhou People's Hospital (Cangzhou, China). The tissues were snap-frozen in liquid nitrogen immediately following resection and stored at -80°C. In addition, information regarding the clinical features (Table I) of the patients was collected from the medical records for study analysis and the pathological grade/tumor node metastasis (TNM) stage was assessed based on the 7th edition of the AJCC Cancer Staging Manual (13). The classification of diseases was performed according to the International Classification of Diseases 10th revision (14).

**Microarray analysis.** Microarray analysis was performed in five pairs of TSCC and Ctrl tissues, which were randomly selected from the total number of specimens of the

enrolled patients (including 3 males and 2 females; mean age, 47.2±8.8 years; age range, 36-58 years). The separation of total RNA in the specimens was performed using TRIzol® reagent (Invitrogen; Thermo Fisher Scientific, Inc.). The integrity and quantification analysis of total RNA was performed using an Agilent 2100 Bioanalyzer (Agilent Technologies, Inc.) and NanoDrop ND-1000 spectrophotometer (Thermo Fisher Scientific, Inc.), respectively. The linear RNAs were removed from the total RNA molecules using RNase R (Epicentre; Illumina, Inc.). Microarray analysis was conducted on the Platform GPL19978 (<https://www.ncbi.nlm.nih.gov/geo/query/acc.cgi?acc=GPL19978>) with the use of Agilent-069978 Arraystar Human CircRNA microarray V1 (Agilent Technologies, Inc.) and the Arraystar Human Circular RNA Microarray V1.0 (6x7K; Arraystar, Inc.), which contains 5,396 probes specific for the human circRNA backsplice junction region. The detailed procedure was performed as described in a previous study (15).

**Bioinformatics analysis.** Differential expression analysis between five TSCC and Ctrl tissues was performed using the Limma package (<https://cran.r-project.org/bin/windows/base/>) in R software v.4.0.2. Principal component analysis (PCA) and heatmap analysis for circRNA expression profiling were conducted using the Factoextra (<https://cran.r-project.org/web/packages/factoextra/index.html>) and pheatmap packages v.4.0.2 (<https://cran.r-project.org/web/packages/pheatmap/index.html>) in the R software. The DEcircRNAs were identified based on the fold change (FC) ≥2.0 and adjusted P-value (BH multiple test correction) <0.05. These indices are shown in the volcano plot. Gene Ontology (GO) (<http://geneontology.org/>) and Kyoto Encyclopedia of Genes and Genomes (KEGG) (<https://david.ncifcrf.gov>) enrichment analyses were performed to identify DEcircRNAs based on the gene location and target miRNAs (miranda criterion, total score >120 & total energy <-20). The circRNA-miRNA regulatory network of the top 10 DEcircRNAs (based on rank of log<sub>2</sub>FC) was predicted by miRanda v.3.3a (<http://www.microrna.org/microrna/getDownloads.do>). The annotation for the target miRNA was obtained from miRwalk database v.3 (<http://mirwalk.umm.uni-heidelberg.de/>), which covered the GO database (molecular function, cellular component and biological process), the pathway database (KEGG database), the human phenotype database (<https://hpo.jax.org/app/>) and the disease database (<http://www.obofoundry.org/ontology/doid.html>).

**Reverse transcription-quantitative PCR (RT-qPCR).** According to the Log<sub>2</sub>FC absolute value, the top five upregulated and downregulated DEcircRNAs were selected as candidate DEcircRNAs for further investigation. RT-qPCR was performed to determine the relative expression levels of 10 candidate circRNAs in tumor and paired Ctrl tissues derived from 60 patients with TSCC. Briefly, total RNA was extracted using TRIzol® reagent (Invitrogen; Thermo Fisher Scientific, Inc.). The detection of circRNAs was performed following digestion of the linear RNA using RNase R (Epicentre; Illumina, Inc.). Subsequently, the synthesis of cDNA was carried out (denaturation at 65°C for 5 min, reverse transcription at 42°C for 18 min and inactivation at 98°C

Table I. Characteristics of patients with TSCC.

| Characteristics                         | Patients with TSCC (n=60) | Female patients (n=17) | Male patients (n=43) |
|---|---------------------------|------------------------|----------------------|
| Age, years (mean ± SD)                  | 56.3±11.1                 | 51.7±11.4              | 58.1±10.6            |
| Age, n (%)                              |                           |                        |                      |
| 18-39 years                             | 4 (6.7)                   | 2 (11.8)               | 2 (4.7)              |
| 40-49 years                             | 9 (15.0)                  | 5 (29.4)               | 4 (9.3)              |
| 50-59 years                             | 24 (40.0)                 | 6 (35.3)               | 18 (41.9)            |
| 60-69 years                             | 16 (26.7)                 | 3 (17.6)               | 13 (30.2)            |
| 70-79 years                             | 7 (11.7)                  | 1 (5.9)                | 6 (14.0)             |
| Sex, n (%)                              |                           |                        |                      |
| Male                                    | 43 (71.7)                 | 0 (0.0)                | 43 (100.0)           |
| Female                                  | 17 (28.3)                 | 17 (100.0)             | 0 (0.0)              |
| Han nationality, n (%)                  | 60 (100.0)                | 17 (100.0)             | 43 (100.0)           |
| Origin, n (%)                           |                           |                        |                      |
| Eastern region of Hebei province, China | 37 (61.7)                 | 11 (64.7)              | 26 (60.5)            |
| Other regions of Hebei province, China  | 18 (30.0)                 | 4 (23.5)               | 14 (32.6)            |
| Other provinces, China                  | 5 (8.3)                   | 2 (11.8)               | 3 (7.0)              |
| Pathological grade, n (%)               |                           |                        |                      |
| G1                                      | 14 (23.3)                 | 5 (29.4)               | 9 (20.9)             |
| G2                                      | 33 (55.0)                 | 9 (52.9)               | 24 (55.8)            |
| G3                                      | 13 (21.7)                 | 3 (17.6)               | 10 (23.3)            |
| ICD-10 classification code, n (%)       |                           |                        |                      |
| C02.1, M8070/31                         | 3 (5.0)                   | 2 (11.8)               | 1 (2.3)              |
| C02.1, M8070/32                         | 8 (13.3)                  | 3 (17.6)               | 5 (11.6)             |
| C02.1, M8070/33                         | 3 (5.0)                   | 0 (0.0)                | 3 (7.0)              |
| C02.8, M8070/31                         | 2 (3.3)                   | 1 (5.9)                | 1 (2.3)              |
| C02.8, M8070/32                         | 5 (8.3)                   | 1 (5.9)                | 4 (9.3)              |
| C02.8, M8070/33                         | 1 (1.7)                   | 1 (5.9)                | 0 (0.0)              |
| C02.9, M8070/31                         | 9 (15.0)                  | 2 (11.8)               | 7 (16.3)             |
| C02.9, M8070/32                         | 20 (33.3)                 | 5 (29.4)               | 15 (34.9)            |
| C02.9, M8070/33                         | 9 (15.0)                  | 2 (11.8)               | 7 (16.3)             |
| T stage, n (%)                          |                           |                        |                      |
| T1                                      | 11 (18.3)                 | 2 (11.8)               | 9 (20.9)             |
| T2                                      | 37 (61.7)                 | 15 (88.2)              | 22 (51.2)            |
| T3                                      | 12 (20.0)                 | 0 (0.0)                | 12 (27.9)            |
| N stage, n (%)                          |                           |                        |                      |
| N0                                      | 43 (71.7)                 | 17 (100.0)             | 26 (60.5)            |
| N1                                      | 13 (21.7)                 | 0 (0.0)                | 13 (30.2)            |
| N2                                      | 4 (6.6)                   | 0 (0.0)                | 4 (9.3)              |
| TNM stage, n (%)                        |                           |                        |                      |
| I                                       | 11 (18.3)                 | 2 (11.8)               | 9 (20.9)             |
| II                                      | 31 (51.7)                 | 15 (88.2)              | 16 (37.2)            |
| III                                     | 14 (23.3)                 | 0 (0.0)                | 14 (32.6)            |
| IV                                      | 4 (6.7)                   | 0 (0.0)                | 4 (9.3)              |
| Adjuvant radiotherapy, n (%)            |                           |                        |                      |
| Yes                                     | 44 (73.3)                 | 10 (58.8)              | 34 (79.1)            |
| No                                      | 16 (26.7)                 | 7 (41.2)               | 9 (20.9)             |

ICD-10, International Classification of Diseases 10th revision (26); TSCC, tongue squamous cell carcinoma.

for 5 min) using the PrimeScript™ RT reagent kit (Takara Bio, Inc.), followed by its amplification using SYBR-Green

Premix DimerEraser™ (Takara Bio, Inc.). Lastly, the relative expression levels of the circRNAs were calculated using

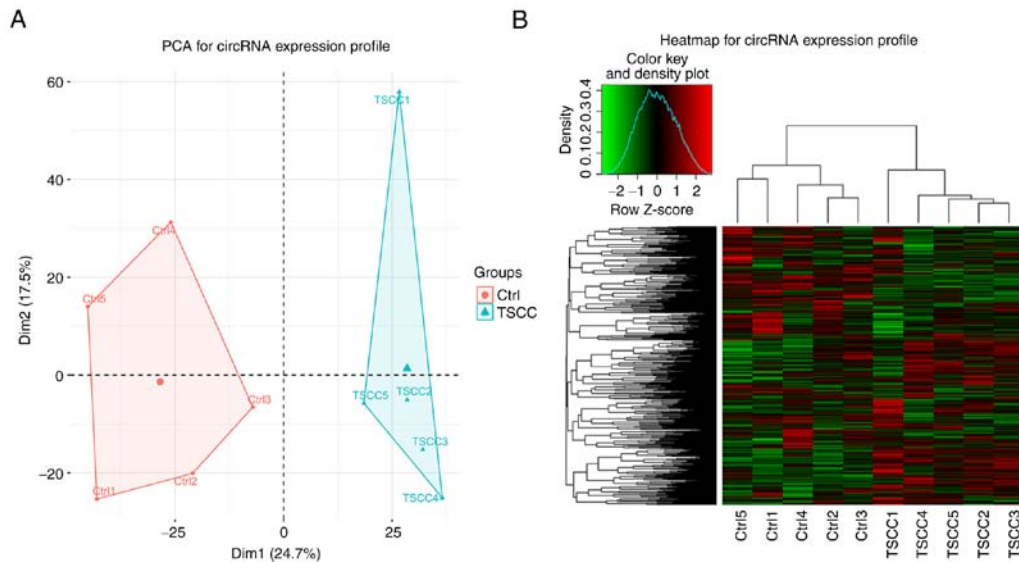


Figure 1. PCA and heatmap analysis. (A) PCA and (B) heatmap analysis of circRNA expression profile in tumor and paired Ctrl tissues derived from patients with TSSC. circRNA, circular RNA; Ctrl, paired adjacent normal tissues; Dim, dimension; PCA, principal component analysis; TSSC, tongue squamous cell carcinoma.

the  $2^{-\Delta\Delta C_q}$  method (16). The thermocycling conditions for qPCR were as follows: Pre-denaturation at 95°C for 3 min; followed by 40 cycles of denaturation at 95°C for 15 sec and annealing/elongation at 61°C for 20 sec. GAPDH was used as an internal reference for circRNAs. The primers are shown in Table SI.

**Survival analysis.** The survival follow-up data of the patients were collected from the records and the last follow-up date was May 31, 2020. Overall survival (OS) was evaluated from the date of surgery to the date of death.

**Statistical analysis.** The estimation of the sample size was performed based on the expression levels of 10 candidate circRNAs in the microarray analysis. All experimental studies were conducted in triplicate. The statistically significant differences in the expression levels of the 10 candidate circRNAs between tumor and Ctrl tissues were evaluated based on a significance level of 0.05 and a power of 0.80. The required sample size included 57 pairs of tumor and Ctrl tissues. Considering an attrition rate of 5%, the final sample size was set to 60 pairs of tumor and Ctrl tissues. Descriptive analysis was performed for the characteristics of the patients, using numbers, percentages or mean  $\pm$  SD. The relative expression levels of circRNAs were presented as the median with the interquartile range and differences in the expression levels between tumor and Ctrl tissues were determined using the Wilcoxon signed-rank test. The correlation analysis between tumor circRNA expression and clinical features was carried out using the Spearman's rank correlation test. A Kaplan-Meier curve was used to display the OS. According to the median level of circRNA expression, the latter was divided into circRNA high and low expression. The association between the expression levels of circRNAs in the tumor samples and OS was evaluated using the log-rank test. SPSS software (v22.0; IBM Corp.) and GraphPad Prism software (v7.01; GraphPad Software, Inc.) were used for data analysis

and graphical presentation.  $P < 0.05$  was considered to indicate a statistically significant difference.

## Results

**Clinical characteristics of patients with TSSC.** A total of 60 patients with TSSC with a mean age of  $56.3 \pm 11.1$  years were included. The number of male and female patients was 43 (71.7%) and 17 (28.3%), respectively (Table I). The evaluation of the pathological grade of the patients yielded the following results: A total of 14 (23.3%) patients presented with G1 TSSC, whereas 33 (55.0%) and 13 (21.7%) exhibited G2 and G3 TSSC tumors, respectively. The TNM stage classification included 11 (18.3%) patients with stage I, 31 (51.7%) patients with stage II, 14 (23.3%) patients with stage III and 4 (6.7%) patients with stage IV tumors. In addition, 44 (73.3%) patients received adjuvant radiotherapy. Detailed information of patients with TSSC in the present study is shown in Table I.

**PCA and heatmap analysis for the evaluation of the circRNA expression profile.** The PCA tool was used to describe protein dynamics and PCA analysis indicated that the DEcircRNAs detected in the TSSC and Ctrl tissues were distributed in two separate parts, suggesting that a clear segregation of the circRNA expression profile was noted between TSSC and Ctrl tissues (Fig. 1A). In the row clustering step, the TSSC tissues were all grouped together to the right side considering their similar DEcircRNA patterns, while the Ctrl tissues were all grouped into the left cluster since their DEcircRNA patterns were more similar, suggesting that circRNA expression profile could differentiate TSSC tissues from Ctrl tissues (Fig. 1B).

**Volcano plot for the circRNA expression profile.** A total of 3,744 circRNAs were detected in more than half of the samples, and were included in the subsequent analysis. The volcano plot indicated 134 upregulated and 67 downregulated DEcircRNAs. A total of 3,543 circRNAs with unaltered

Table II. Top 10 DEcircRNAs, including top five downregulated DEcircRNAs and top five upregulated DEcircRNAs.

| circRNA      | Probe name  | Chr   | Symbol  | Log <sub>2</sub> (FC) | P-value              | P <sub>adj</sub> value | Trend |
|--------------|-------------|-------|---------|-----------------------|----------------------|------------------------|-------|
| circ_0020048 | ASCRP001058 | chr10 | TCF7L2  | 5.002                 | 6.7x10 <sup>-6</sup> | 1.7x10 <sup>-3</sup>   | Up    |
| circ_0000919 | ASCRP000027 | chr19 | ATP13A1 | 3.728                 | 3.2x10 <sup>-6</sup> | 1.4x10 <sup>-3</sup>   | Up    |
| circ_0004525 | ASCRP003285 | chr20 | RBCK1   | 3.526                 | 5.7x10 <sup>-7</sup> | 7.6x10 <sup>-4</sup>   | Up    |
| circ_0066887 | ASCRP003739 | chr3  | GSK3B   | 3.526                 | 3.1x10 <sup>-4</sup> | 1.6x10 <sup>-2</sup>   | Up    |
| circ_0002113 | ASCRP003424 | chr21 | IFNGR2  | 3.364                 | 3.7x10 <sup>-4</sup> | 1.8x10 <sup>-2</sup>   | Up    |
| circ_0004029 | ASCRP003104 | chr2  | UXS1    | -7.482                | 3.1x10 <sup>-7</sup> | 7.6x10 <sup>-4</sup>   | Down  |
| circ_0004503 | ASCRP004245 | chr5  | UBE2D2  | -7.361                | 7.7x10 <sup>-6</sup> | 1.7x10 <sup>-3</sup>   | Down  |
| circ_0008752 | ASCRP004812 | chr8  | CNOT7   | -5.871                | 2.4x10 <sup>-6</sup> | 1.4x10 <sup>-3</sup>   | Down  |
| circ_0002300 | ASCRP004304 | chr5  | CANX    | -5.133                | 8.2x10 <sup>-4</sup> | 2.8x10 <sup>-2</sup>   | Down  |
| circ_0001811 | ASCRP004898 | chr8  | STAU2   | -4.991                | 7.5x10 <sup>-5</sup> | 7.8x10 <sup>-3</sup>   | Down  |

Top 10 DEcircRNAs were selected by ranking of absolute value of Log<sub>2</sub>(FC). Chr, chromosome; circRNA/circ, circular RNA; DE, differentially expressed; Down, downregulated; FC, fold change; P<sub>adj</sub> value, adjusted P-value; Up, upregulated.

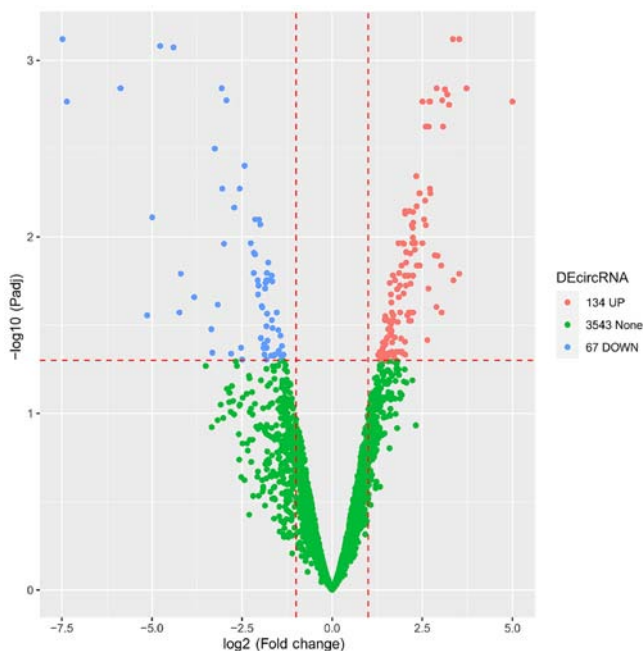


Figure 2. Volcano plot of the circRNA expression profile noted in tongue squamous cell carcinoma and paired adjacent tissues. circRNA, circular RNA; DEcircRNA, differentially expressed circRNA; DOWN, downregulated; P<sub>adj</sub>, adjusted P-value; UP, upregulated.

expression levels were noted in the TSCC tissues compared with the Ctrl tissues (Fig. 2).

**GO and KEGG enrichment analysis of DEcircRNAs.** GO and KEGG enrichment analysis was performed. GO enrichment analysis was performed based on specific gene functions and the data indicated that DEcircRNAs were enriched in molecular functions, including ‘protein binding’, ‘ATP binding’ and ‘protein kinase activity’, cellular components, including ‘neuronal cell body’, ‘cytosol’ and ‘nucleoplasm’, and biological processes, including ‘regulation of angiogenesis’, ‘positive regulation of angiogenesis’ and ‘canonical Wnt signaling pathway’ based on significance (Fig. 3A). In addition,

GO enrichment analysis was performed based on target miRNAs and the results indicated that DEcircRNAs were enriched in molecular functions including ‘TGF-β activation’, ‘insulin like growth receptor binding’ and ‘channel activity’, and cellular components including ‘receptor complex’, ‘Schmidt-Lanterman incisures’ and ‘secretory granule’, and biological processes, including ‘response to nicotine’, ‘organ growth’ and ‘B cell homeostasis’ based on significance (Fig. 3B). KEGG enrichment analysis was performed for DEcircRNAs based on specific gene functions and the data demonstrated that DEcircRNAs were enriched in the ‘MAPK signaling pathway’, ‘Wnt signaling pathway’ and ‘Ras signaling pathway’ based on significance (Fig. 3C). Furthermore, KEGG enrichment analysis was performed for DEcircRNAs based on target miRNAs. The data demonstrated that DEcircRNAs were enriched in the ‘TGF beta signaling pathway’, ‘Complement and coagulation cascades’ and ‘Cytokine cytokine receptor interaction’ based on significance (Fig. 3D).

**Regulatory network of circRNA-miRNA interactions.** The top 10 candidate DEcircRNAs comprised the top five upregulated and the top five downregulated DEcircRNAs, which were detected in five TSCC and Ctrl tissues. These circRNAs were screened based on the log<sub>2</sub>FC value (Table II). A circRNA-miRNA regulatory network of the top 10 DEcircRNAs was established using the miRanda database (Fig. 4). circ\_0066887 was predicted not to bind to a miRNA target, whereas the following DEcircRNAs demonstrated multiple (≥3) target miRNAs: circ\_0020048, circ\_0000919, circ\_0004525, circ\_0002113, circ\_0004029, circ\_0004503, circ\_0008752, circ\_0002300 and circ\_0001811.

**Validation of candidate DEcircRNA expression in TSCC tissues.** The expression levels of 10 candidate DEcircRNAs were further assessed in the tumor and paired Ctrl tissues of 60 patients with TSCC using RT-qPCR analysis. The expression levels of circ\_0020048, circ\_0000919, circ\_0004525 (Fig. 5A-C; all P<0.001) and circ\_0002113 (Fig. 5E; P<0.001) were increased in TSCC tumor tissues compared with in Ctrl tissues, while the expression levels of circ\_0004029,

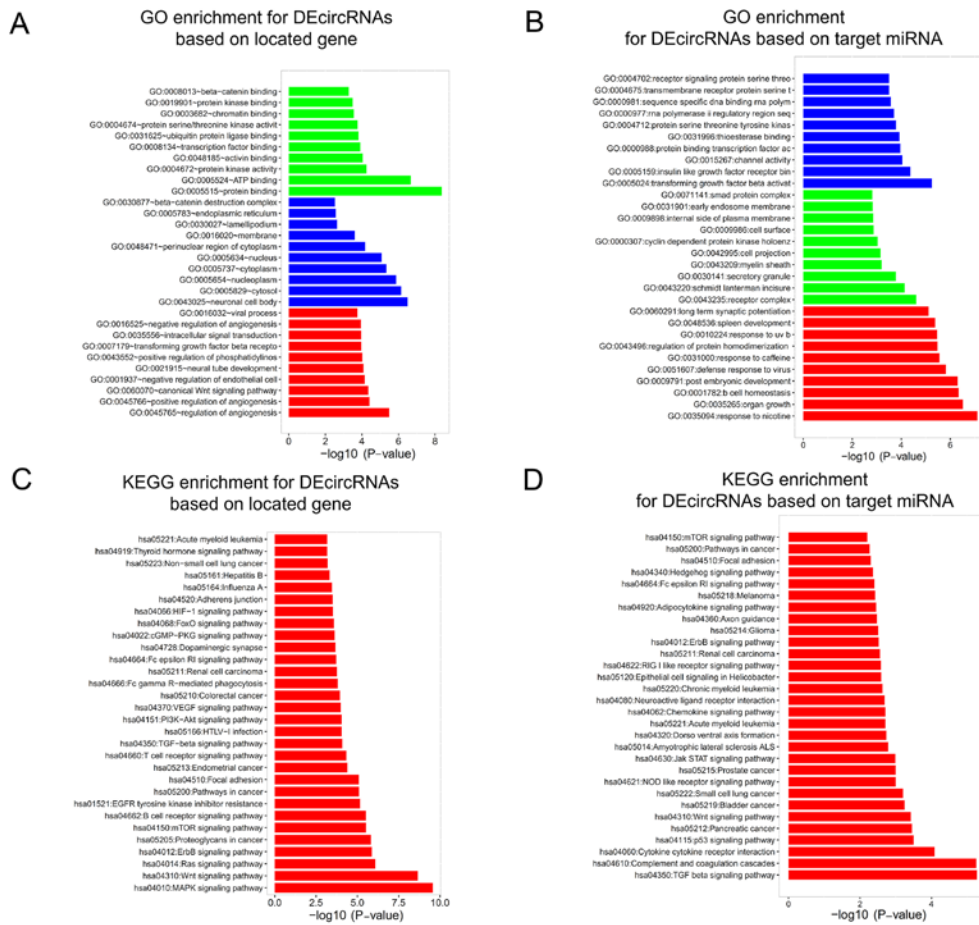


Figure 3. Enrichment analysis. GO enrichment analysis of DEcircRNAs based on (A) the gene function and (B) the target miRNA in patients with TSCC. KEGG enrichment analysis for DEcircRNAs based on (C) the gene function and (D) the target miRNA in patients with TSCC. circRNA, circular RNA; DE, differentially expressed; GO, Gene Ontology; KEGG, Kyoto Encyclopedia of Genes and Genomes; miRNA; microRNA; TSCC; tongue squamous cell carcinoma.

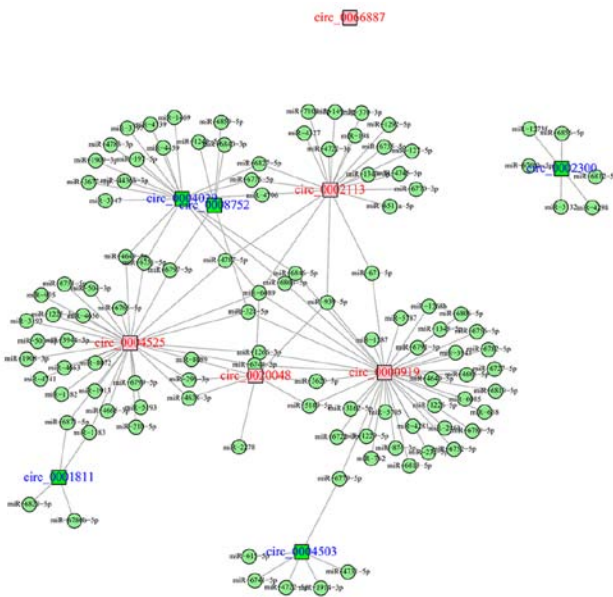


Figure 4. Network of circRNA-miRNA interactions. Interaction of top 10 candidate differentially expressed circRNAs with their potential target miRNAs in tongue squamous cell carcinoma. The heatmap is a graphical presentation of the data composed of grids of colors and clusters on both rows and columns and provides an overview of the numerical differences. Squares indicate the circRNAs and circles indicate miRNAs. circRNAs in red are upregulated circRNAs; circRNAs in blue are downregulated circRNAs; miRNAs in green are the potential targets of circRNAs. circRNA/circ, circular RNA; miRNA/miR, microRNA.

circ\_0004503 (Fig. 5F and G; both  $P < 0.001$ ), circ\_0008752 (Fig. 5H;  $P = 0.002$ ), circ\_0002300 (Fig. 5I;  $P < 0.001$ ) and circ\_0001811 (Fig. 5J;  $P = 0.005$ ) were decreased in TSCC tumor tissues compared with in Ctrl tissues. The expression levels of circ\_0066887 were similar between TSCC tumor tissues and Ctrl tissues (Fig. 5D;  $P = 0.131$ ).

*Association between the expression levels of candidate DEcircRNAs and tumor features in patients with TSCC.* The association between the expression levels of candidate tumor DEcircRNAs and tumor features was further detected in patients with TSCC (Table III). The expression levels of circ\_0020048 in tumor tissues exhibited a positive association with T stage ( $P = 0.010$ ) and TNM stage ( $P = 0.006$ ). The expression levels of circ\_0000919 exhibited a positive association with T stage ( $P = 0.022$ ), N stage ( $P < 0.001$ ) and TNM stage ( $P < 0.001$ ). In contrast to these findings, the expression levels of circ\_0004503 in the tumor tissues were negatively associated with pathological grade ( $P = 0.015$ ), whereas those of circ\_0008752 were negatively associated with pathological grade ( $P = 0.024$ ) and N stage ( $P = 0.036$ ). The expression levels of circ\_0002300 noted in the tumor samples were negatively associated with pathological grade ( $P = 0.048$ ), N stage ( $P = 0.048$ ) and TNM stage ( $P = 0.021$ ). The expression levels of other candidate DEcircRNAs were not associated with tumor

Table III. Associations between candidate differentially expressed circRNAs and clinical features were determined using Spearman's rank sum test.

| Characteristics           | circ_0020048, median (IQR) | circ_0000919, median (IQR) | circ_0004525, median (IQR) | circ_0066887, median (IQR) | circ_0002113, median (IQR) | circ_0004029, median (IQR) | circ_0004503, median (IQR) | circ_0008752, median (IQR) | circ_0002300, median (IQR) | circ_0001811, median (IQR) |
|---------------------------|----------------------------|----------------------------|----------------------------|----------------------------|----------------------------|----------------------------|----------------------------|----------------------------|----------------------------|----------------------------|
| <b>Pathological grade</b> |                            |                            |                            |                            |                            |                            |                            |                            |                            |                            |
| G1                        | 1.898<br>(1.117-2.779)     | 2.853<br>(1.389-3.597)     | 2.502<br>(1.548-3.206)     | 1.100<br>(0.563-2.137)     | 1.280<br>(0.986-2.806)     | 0.384<br>(0.193-0.918)     | 0.561<br>(0.278-1.190)     | 0.800<br>(0.419-1.465)     | 0.502<br>(0.376-1.047)     | 0.509<br>(0.265-0.793)     |
| G2                        | 3.310<br>(2.290-4.836)     | 3.360<br>(2.554-4.295)     | 1.781<br>(1.159-2.980)     | 1.449<br>(0.771-2.213)     | 1.729<br>(0.981-3.207)     | 0.281<br>(0.151-0.477)     | 0.359<br>(0.285-0.712)     | 0.553<br>(0.420-0.833)     | 0.414<br>(0.279-0.580)     | 0.667<br>(0.525-0.919)     |
| G3                        | 2.231<br>(1.335-3.644)     | 3.410<br>(2.499-4.287)     | 2.260<br>(1.281-3.844)     | 1.068<br>(0.799-2.002)     | 1.868<br>(1.390-3.051)     | 0.306<br>(0.100-0.536)     | 0.250<br>(0.194-0.391)     | 0.387<br>(0.309-0.488)     | 0.310<br>(0.236-0.590)     | 0.650<br>(0.421-0.924)     |
| P-value                   | 0.539                      | 0.100                      | 0.628                      | 0.844                      | 0.249                      | 0.224                      | 0.015                      | 0.024                      | 0.048                      | 0.334                      |
| <b>T stage</b>            |                            |                            |                            |                            |                            |                            |                            |                            |                            |                            |
| T1                        | 1.497<br>(1.165-2.448)     | 2.907<br>(2.008-3.189)     | 1.897<br>(1.175-2.514)     | 1.503<br>(0.576-2.372)     | 1.729<br>(0.751-2.043)     | 0.400<br>(0.184-0.756)     | 0.322<br>(0.286-0.851)     | 0.685<br>(0.465-0.895)     | 0.545<br>(0.407-1.035)     | 0.740<br>(0.583-1.408)     |
| T2                        | 2.855<br>(1.501-4.160)     | 3.392<br>(2.323-4.069)     | 2.310<br>(1.332-3.095)     | 0.982<br>(0.757-1.649)     | 1.772<br>(1.073-3.215)     | 0.306<br>(0.145-0.504)     | 0.349<br>(0.266-0.612)     | 0.491<br>(0.375-1.091)     | 0.413<br>(0.269-0.580)     | 0.642<br>(0.463-0.959)     |
| T3                        | 3.678<br>(2.014-4.647)     | 3.740<br>(3.157-4.410)     | 2.371<br>(1.390-3.666)     | 1.830<br>(0.970-2.869)     | 1.602<br>(1.093-3.209)     | 0.257<br>(0.179-0.443)     | 0.292<br>(0.209-0.649)     | 0.523<br>(0.321-0.750)     | 0.322<br>(0.190-0.660)     | 0.518<br>(0.336-0.673)     |
| P-value                   | 0.010                      | 0.022                      | 0.386                      | 0.299                      | 0.485                      | 0.288                      | 0.312                      | 0.472                      | 0.084                      | 0.081                      |
| <b>N stage</b>            |                            |                            |                            |                            |                            |                            |                            |                            |                            |                            |
| N0                        | 2.379<br>(1.260-4.094)     | 2.907<br>(2.211-3.634)     | 2.260<br>(1.308-2.977)     | 1.218<br>(0.750-2.053)     | 1.772<br>(0.957-3.125)     | 0.322<br>(0.166-0.575)     | 0.349<br>(0.286-0.697)     | 0.591<br>(0.400-0.949)     | 0.447<br>(0.310-0.634)     | 0.650<br>(0.479-1.065)     |
| N1                        | 3.310<br>(2.086-4.170)     | 3.946<br>(3.558-4.679)     | 1.493<br>(1.047-4.052)     | 1.488<br>(1.108-2.463)     | 1.659<br>(1.064-2.949)     | 0.249<br>(0.147-0.558)     | 0.250<br>(0.203-0.831)     | 0.441<br>(0.343-0.730)     | 0.365<br>(0.241-0.627)     | 0.542<br>(0.339-0.680)     |
| N2                        | 2.922<br>(2.815-4.320)     | 4.006<br>(3.217-5.404)     | 3.047<br>(2.065-4.453)     | 0.830<br>(0.369-1.817)     | 1.866<br>(1.267-3.345)     | 0.179<br>(0.141-0.252)     | 0.412<br>(0.263-0.571)     | 0.319<br>(0.198-0.447)     | 0.251<br>(0.226-0.283)     | 0.689<br>(0.354-0.737)     |
| P-value                   | 0.082                      | <0.001                     | 0.316                      | 0.402                      | 0.845                      | 0.221                      | 0.235                      | 0.036                      | 0.048                      | 0.138                      |
| <b>TNM stage</b>          |                            |                            |                            |                            |                            |                            |                            |                            |                            |                            |
| I                         | 1.497<br>(1.165-2.448)     | 2.907<br>(2.008-3.189)     | 1.897<br>(1.175-2.514)     | 1.503<br>(0.576-2.372)     | 1.729<br>(0.751-2.043)     | 0.400<br>(0.184-0.756)     | 0.322<br>(0.286-0.851)     | 0.685<br>(0.465-0.895)     | 0.545<br>(0.407-1.035)     | 0.740<br>(0.583-1.408)     |
| II                        | 2.639<br>(1.263-4.908)     | 2.967<br>(2.211-3.639)     | 2.281<br>(1.308-3.045)     | 0.977<br>(0.750-1.743)     | 1.772<br>(0.957-3.324)     | 0.322<br>(0.154-0.505)     | 0.349<br>(0.272-0.614)     | 0.567<br>(0.399-1.422)     | 0.434<br>(0.265-0.619)     | 0.642<br>(0.447-1.065)     |
| III                       | 3.350<br>(2.159-4.263)     | 3.939<br>(3.394-4.547)     | 2.227<br>(1.204-3.864)     | 1.644<br>(1.128-2.694)     | 1.694<br>(1.064-3.058)     | 0.286<br>(0.158-0.512)     | 0.271<br>(0.204-0.762)     | 0.482<br>(0.353-0.710)     | 0.399<br>(0.272-0.593)     | 0.554<br>(0.341-0.683)     |
| IV                        | 2.922<br>(2.815-4.320)     | 4.006<br>(3.217-5.404)     | 3.047<br>(2.065-4.453)     | 0.830<br>(0.369-1.817)     | 1.866<br>(1.267-3.345)     | 0.179<br>(0.141-0.252)     | 0.412<br>(0.263-0.571)     | 0.319<br>(0.198-0.447)     | 0.251<br>(0.226-0.283)     | 0.689<br>(0.354-0.737)     |
| P-value                   | 0.006                      | <0.001                     | 0.183                      | 0.524                      | 0.355                      | 0.140                      | 0.321                      | 0.062                      | 0.021                      | 0.118                      |

circRNA/circ, circular RNA; IQR, interquartile range.

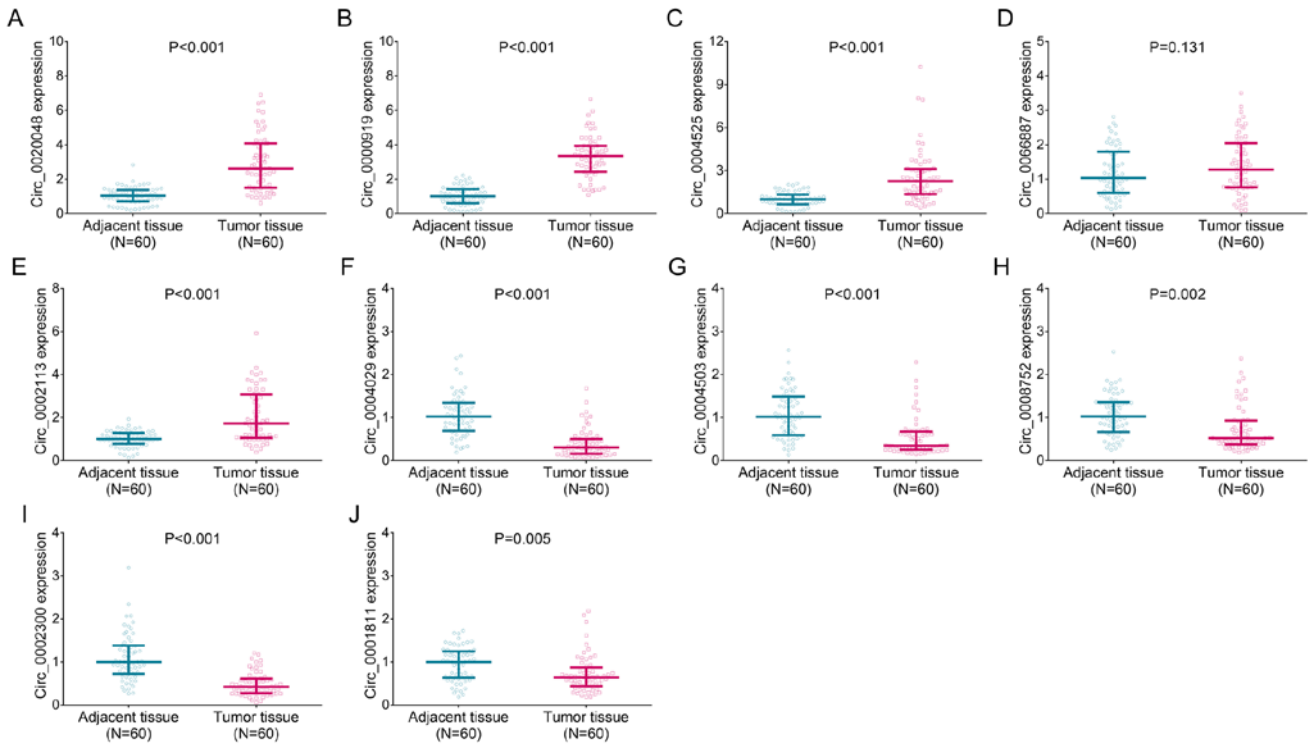


Figure 5. Validation of candidate differentially expressed circRNA expression levels in patients with TSCC. Comparison of the expression levels of (A) circ\_0020048, (B) circ\_0000919, (C) circ\_0004525, (D) circ\_0066887, (E) circ\_0002113, (F) circ\_0004029, (G) circ\_0004503, (H) circ\_0008752, (I) circ\_0002300 and (J) circ\_0001811 between 60 TSCC and adjacent tissues. circRNA/circ, circular RNA; TSCC, tongue squamous cell carcinoma.

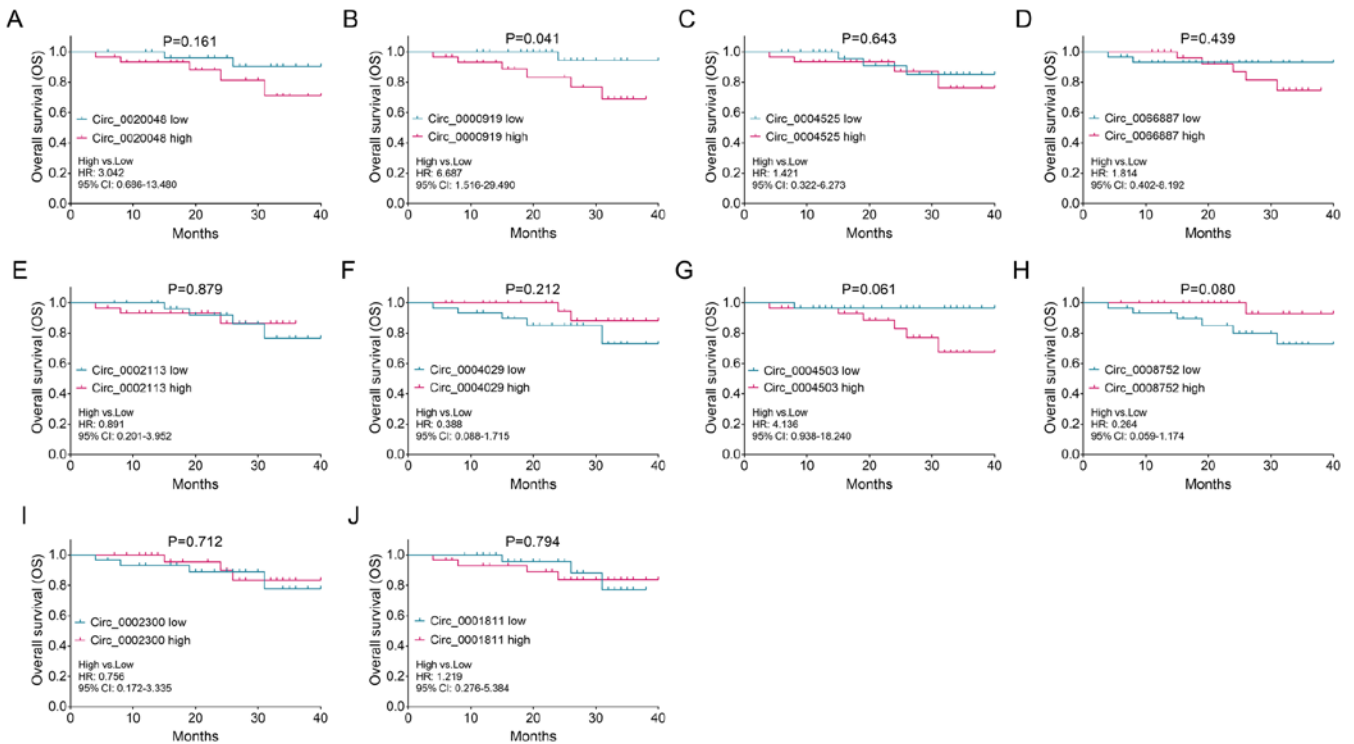


Figure 6. Association between candidate differentially expressed circRNAs and prognosis of patients with TSCC. Association between the expression levels of (A) circ\_0020048, (B) circ\_0000919, (C) circ\_0004525, (D) circ\_0066887, (E) circ\_0002113, (F) circ\_0004029, (G) circ\_0004503, (H) circ\_0008752, (I) circ\_0002300 and (J) circ\_0001811 in tumors derived from 60 patients with TSCC and overall survival. 95% CI, 95% confidence interval; circRNA/circ, circular RNA; HR, hazard ratio; OS, overall survival; TSCC, tongue squamous cell carcinoma.

features, including pathological grade, T stage, N stage and TNM stage (all  $P > 0.05$ ).

*Association between the expression levels of candidate DEcircRNAs and prognosis of patients with TSCC. To*



Table IV. Summary of study findings.

| circRNAs     | Significant difference<br>Tumor vs. adjacent | Significant association |         |         |           |     |
|--------------|--|-------------------------|---------|---------|-----------|-----|
|              |  | Pathological grade      | T stage | N stage | TNM stage | OS  |
| circ_0020048 | Yes  | No                      | Yes     | No      | Yes       | No  |
| circ_0000919 | Yes  | No                      | Yes     | Yes     | Yes       | Yes |
| circ_0004525 | Yes  | No                      | No      | No      | No        | No  |
| circ_0066887 | No   | No                      | No      | No      | No        | No  |
| circ_0002113 | Yes  | No                      | No      | No      | No        | No  |
| circ_0004029 | Yes  | No                      | No      | No      | No        | No  |
| circ_0004503 | Yes  | Yes                     | No      | No      | No        | No  |
| circ_0008752 | Yes  | Yes                     | No      | Yes     | No        | No  |
| circ_0002300 | Yes  | Yes                     | No      | Yes     | Yes       | No  |
| circ_0001811 | Yes  | No                      | No      | No      | No        | No  |

circRNA/circ, circular RNA; OS, overall survival.

explore the potential prognostic value of the top 10 candidate DEcircRNAs in TSCC, the association of their corresponding expression levels with OS time was assessed. The higher expression levels of circ\_0000919 in tumor tissues were associated with decreased OS time in patients with TSCC (Fig. 6B;  $P=0.041$ ), while no association was observed between the expression levels of the other DEcircRNAs, including circ\_0020048 (Fig. 6A), circ\_0004525 circ\_0066887, circ\_0002113, circ\_0004029, circ\_0004503, circ\_0008752, circ\_0002300 and circ\_0001811 (Fig. 6C-J), and the OS time of patients with TSCC (all  $P>0.05$ ).

The data regarding the comparison of the expression levels of the 10 candidate DEcircRNAs between tumor and Ctrl tissues, as well as their corresponding association with tumor features and OS time are summarized in Table IV. Among the 10 candidate DEcircRNAs, the expression levels of circ\_0000919 were increased in TSCC tumor tissues compared with in the Ctrl tissues and associated with higher TNM stage and low OS time of patients with TSCC, suggesting that circ\_0000919 could be used as a diagnostic and prognostic biomarker in TSCC.

## Discussion

circRNAs are expressed in the cytoplasm of eukaryotic cells and display high enrichment, stability and diversity (17,18). They also exhibit tissue- and developmental phase-specific expression (17,18). circRNAs possess unique structures and high specificity (8). Furthermore, they exert diverse regulatory functions and present potential value as diagnostic and prognostic markers in multiple cancer cells, including cancer cells, immune cells, hematopoietic stem cells, etc. (18,19). In addition, the application of microarray-based technologies has increased the understanding of the diverse functions of circRNAs (17). Their contributions in carcinogenesis have attracted considerable attention (17). Therefore, a high number of circRNAs and their potential functions as cancer-associated regulators have been identified (20). However, studies investigating the circRNA expression profile in TSCC are limited.

Specific circRNAs, including circ\_0001742 and circ\_081069, are involved in the development of TSCC (11,12). Therefore, the present study aimed to identify the comprehensive circRNA expression profile associated with TSCC. The findings may provide additional evidence regarding the role of circRNAs in TSCC.

In the present study, microarray and bioinformatics analyses were conducted in five pairs of TSCC and Ctrl tissues. The data revealed 134 upregulated DEcircRNAs and 67 down-regulated DEcircRNAs in TSCC tissues compared with Ctrl tissues, suggesting that these DEcircRNAs may be involved in the development of TSCC. Additional GO and KEGG enrichment analysis demonstrated that these DEcircRNAs were enriched in tumor-associated biological processes, including 'regulation of angiogenesis' and the 'canonical Wnt signaling pathway', as well as in several oncogenic signaling pathways, such as the 'Wnt signaling pathway', 'MAPK signaling pathway' and 'Ras signaling pathway'. These results may be interpreted in several ways. First, DEcircRNAs may activate angiogenic factors, which further contribute to an active angiogenic state and promote TSCC development. This was based on the existing evidence that angiogenesis is the process of generating new blood vessels required for sufficient nutrition and oxygen supply and tumor growth (18). Second, it was hypothesized that DEcircRNAs may regulate the oncogenic components of the Wnt signaling pathway, such as adenomatous polyposis coli and  $\beta$ -catenin, and lead to its stimulation, which promotes TSCC cell differentiation and survival and enhances TSCC development (21). This was based on previous studies demonstrating that the activation of the Wnt signaling pathway is associated with oncogenic properties of cancer stem cells and the progression of EMT (21,22). Third, it was suggested that DEcircRNAs may regulate the components of the MAPK signaling pathways, leading to excessive activation of proteins and kinases of the Ras signaling pathway, which in turn will affect the development of TSCC. This conclusion was based on the ability of the MAPK cascade to regulate a wide range of cellular processes, including differentiation and apoptosis (20). The MAPK signaling pathway is implicated

in the differentiation and survival of TSCC cells via interaction with other signaling pathways, such as the Ras and ERK signaling pathways (23). Furthermore, this finding was in line with the observation that DEcircRNAs were enriched in the Ras signaling pathway.

In the present study, the top five upregulated and down-regulated DEcircRNAs were selected as candidates for RT-qPCR validation in a total of 60 patients with TSCC. Notably, circ\_0000919 exhibited a positive association with T stage and it could be used to predict low OS in patients with TSCC. The results suggested the potential of circ\_0000919 as a TSCC diagnostic and prognostic biomarker, which may aid disease screening and monitoring of patients with TSCC. The possible explanations for these conclusions are as follows: First, circ\_0000919 may serve as the sponge of several antitumor miRNAs, such as miR-1587 and miR-1226-3p, which in turn may mediate TSCC cell repair capacity and proliferation, as well as radiosensitivity of these tumors (24,25). Therefore, it was suggested that the expression levels of circ\_0000919 were associated with increased TNM stage and unfavorable survival due to its ability to serve as a sponge of antitumor miRNAs. Furthermore, circ\_0000919 may enhance translation efficiency of certain TSCC stimulators or inhibit the translation of several tumor suppressors via protein carrier functions, thereby promoting TSCC tumor development and resulting in poor prognosis of patients with TSCC (17).

However, the present study had several limitations. Firstly, the sample size for candidate DEcircRNA validation was 60, which may lead to limited statistical power. The patients were enrolled in one hospital, which may also contribute to selection bias. Secondly, the present study was a retrospective study and the information regarding tumor recurrence was not recorded in detail in the majority of patients with TSCC. Therefore, the association of candidate DEcircRNAs with disease-free survival was not assessed. Thirdly, in the present study, circ\_0000919 was demonstrated to have diagnostic and prognostic value as a biomarker of TSCC. However, the detailed mechanism of the involvement of circ\_0000919 in TSCC progression requires further investigation in *in vivo* and *in vitro* studies. Furthermore, the top five upregulated and downregulated DEcircRNAs were selected as candidate DEcircRNAs based on the absolute value of log<sub>2</sub>FC for further RT-qPCR validation in 60 patients with TSCC, since these DEcircRNAs were predicted to be novel and promising biomarkers for early screening and follow-up of these patients. RT-qPCR analysis was not conducted to validate all DEcircRNAs based on the microarray data of the 60 patients with TSCC to avoid unnecessary cost. Finally, in the present study, tissue specimens were collected for detection and the data demonstrated that circ\_0000919 may be a candidate TSCC biomarker. Considering that blood samples are more easily collected compared with tissue samples, whether the value of circ\_0000919 in blood samples is the same as that in tissue samples requires additional experimental exploration.

In summary, the present study demonstrated an aberrant circRNA expression profile and potential circRNA-miRNA interactions in TSCC and further identified that circ\_0000919 expression was associated with tumor features. The expression levels of this circRNA could be used to predict unfavorable

OS. These findings suggested that circ\_0000919 may be used as a candidate biomarker for disease management of TSCC.

### Acknowledgements

Not applicable.

### Funding

No funding was received.

### Availability of data and materials

All data generated or analyzed during this study are included in this published article.

### Authors' contributions

HL contributed to the study design. HL, QL, HQ, FD and YQ made substantial contributions to acquisition and interpretation of data. HL, QL and HQ contributed to data analysis and presentation. HL, QL, HQ, FD and YQ were involved in drafting the manuscript and revising it for important intellectual content. HL and QL confirmed the authenticity of all the raw data. All authors read and approved the final manuscript.

### Ethics approval and consent to participate

The present study was approved by the Ethics Committee of Cangzhou Medical College (Cangzhou, China) with the approval no. '20190611-3'. Written informed consent was provided by each eligible patient or his/her guardian if the patients were dead when the clinical data was collected.

### Patient consent for publication

Not applicable.

### Competing interests

The authors declare that they have no competing interests.

### References

1. Kim YJ and Kim JH: Increasing incidence and improving survival of oral tongue squamous cell carcinoma. *Sci Rep* 10: 7877, 2020.
2. Shrestha AD, Vedsted P, Kallestrup P and Neupane D: Prevalence and incidence of oral cancer in low- and middle-income countries: A scoping review. *Eur J Cancer Care (Engl)* 29: e13207, 2020.
3. Ohta K and Yoshimura H: Squamous cell carcinoma of the dorsal tongue. *CMAJ* 191: E1310, 2019.
4. Machiels JP, René Leemans C, Golusinski W, Grau C, Licitra L and Gregoire V; EHNS Executive Board. Electronic address: secretariat@ehns.org; ESMO Guidelines Committee. Electronic address: clinicalguidelines@esmo.org; ESTRO Executive Board. Electronic address: info@estro.org: Squamous cell carcinoma of the oral cavity, larynx, oropharynx and hypopharynx: EHNS-ESMO-ESTRO Clinical Practice Guidelines for diagnosis, treatment and follow-up. *Ann Oncol* 31: 1462-1475, 2020.
5. Okubo M, Iwai T, Nakashima H, Koizumi T, Oguri S, Hirota M, Mitsudo K and Tohna I: Squamous Cell Carcinoma of the Tongue Dorsum: Incidence and Treatment Considerations. *Indian J Otolaryngol Head Neck Surg* 69: 6-10, 2017.

6. Montero PH and Patel SG: Cancer of the oral cavity. *Surg Oncol Clin N Am* 24: 491-508, 2015.
7. Ge P, Zhang J, Zhou L, Lv MQ, Li YX, Wang J and Zhou DX: CircRNA expression profile and functional analysis in testicular tissue of patients with non-obstructive azoospermia. *Reprod Biol Endocrinol* 17: 100, 2019.
8. Kristensen LS, Andersen MS, Stagsted LVW, Ebbesen KK, Hansen TB and Kjems J: The biogenesis, biology and characterization of circular RNAs. *Nat Rev Genet* 20: 675-691, 2019.
9. Fan HY, Jiang J, Tang YJ, Liang XH and Tang YL: circRNAs: A New Chapter in Oral Squamous Cell Carcinoma Biology. *OncoTargets Ther* 13: 9071-9083, 2020.
10. Wang YF, Li BW, Sun S, Li X, Su W, Wang ZH, Wang F, Zhang W and Yang HY: Circular RNA Expression in Oral Squamous Cell Carcinoma. *Front Oncol* 8: 398, 2018.
11. Yao Y, Bi L and Zhang C: Circular RNA\_0001742 has potential to predict advanced tumor stage and poor survival profiles in tongue squamous cell carcinoma management. *J Clin Lab Anal* 34: e23330, 2020.
12. Wei T, Ye P, Yu GY and Zhang ZY: Circular RNA expression profiling identifies specific circular RNAs in tongue squamous cell carcinoma. *Mol Med Rep* 21: 1727-1738, 2020.
13. Edge SB and Compton CC: The American Joint Committee on Cancer: the 7th edition of the AJCC cancer staging manual and the future of TNM. *Ann Surg Oncol* 17: 1471-1474, 2010.
14. World Health Organization: The ICD-10 classification of mental and behavioural disorders: diagnostic criteria for research. World Health Organization, Geneva, Switzerland, 1993. <https://apps.who.int/iris/handle/10665/37108>. Accessed October 25, 2016.
15. Dang Y, Ouyang X, Zhang F, Wang K, Lin Y, Sun B, Wang Y, Wang L and Huang Q: Circular RNAs expression profiles in human gastric cancer. *Sci Rep* 7: 9060, 2017.
16. Livak KJ and Schmittgen TD: Analysis of relative gene expression data using real-time quantitative PCR and the 2(-Delta Delta C(T)) Method. *Methods* 25: 402-408, 2001.
17. Prats AC, David F, Diallo LH, Roussel E, Tatin F, Garmy-Susini B and Lacazette E: Circular RNA, the Key for Translation. *Int J Mol Sci* 21: E8591, 2020.
18. Tucker D, Zheng W, Zhang DH and Dong X: Circular RNA and its potential as prostate cancer biomarkers. *World J Clin Oncol* 11: 563-572, 2020.
19. Lu J, Wang YH, Yoon C, Huang XY, Xu Y, Xie JW, Wang JB, Lin JX, Chen QY, Cao LL, *et al*: Circular RNA circ-RanGAP1 regulates VEGFA expression by targeting miR-877-3p to facilitate gastric cancer invasion and metastasis. *Cancer Lett* 471: 38-48, 2020.
20. Lei M, Zheng G, Ning Q, Zheng J and Dong D: Translation and functional roles of circular RNAs in human cancer. *Mol Cancer* 19: 30, 2020.
21. Martin-Orozco E, Sanchez-Fernandez A, Ortiz-Parra I and Ayala-San Nicolas M: WNT Signaling in Tumors: The Way to Evade Drugs and Immunity. *Front Immunol* 10: 2854, 2019.
22. Basu S, Cheriyaundath S and Ben-Ze'ev A: Cell-cell adhesion: Linking Wnt/ $\beta$ -catenin signaling with partial EMT and stemness traits in tumorigenesis. *Front Oncol* 7: 7, 2018.
23. Guo YJ, Pan WW, Liu SB, Shen ZF, Xu Y and Hu LL: ERK/MAPK signalling pathway and tumorigenesis. *Exp Ther Med* 19: 1997-2007, 2020.
24. Liu R, Shen L, Lin C, He J, Wang Q, Qi Z, Zhang Q, Zhou M and Wang Z: MiR-1587 Regulates DNA Damage Repair and the Radiosensitivity of CRC Cells via Targeting LIG4. *Dose Response* 18: 1559325820936906, 2020.
25. Park EJ, Jung HJ, Choi HJ, Jang HJ, Park HJ, Nejsun LN and Kwon TH: Exosomes co-expressing AQP5-targeting miRNAs and IL-4 receptor-binding peptide inhibit the migration of human breast cancer cells. *FASEB J* 34: 3379-3398, 2020.



This work is licensed under a Creative Commons Attribution-NonCommercial-NoDerivatives 4.0 International (CC BY-NC-ND 4.0) License.